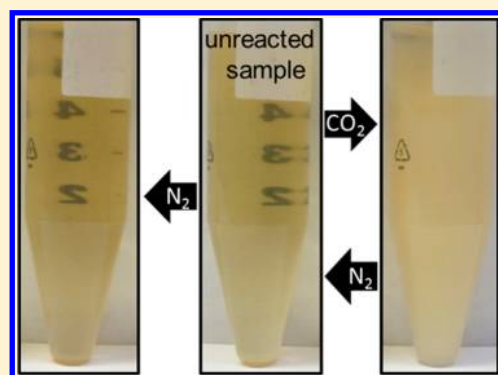


CO₂-Responsive Microemulsions Based on Reactive Ionic LiquidsPaul Brown,[†] Matthew J. Wasbrough,[‡] Burcu E. Gurkan,[†] and T. Alan Hatton^{*,†}[†]Department of Chemical Engineering, Massachusetts Institute of Technology, 77 Massachusetts Avenue, Cambridge, Massachusetts 02139, United States[‡]NIST Centre for Neutron Research, National Institute of Standards and Technology, 100 Bureau Drive, MS 6100, Gaithersburg, Maryland 20899-6100, United States

S Supporting Information

ABSTRACT: We demonstrate that the nanodomains within a ternary system consisting of oil, surfactant, and a new reactive ionic liquid can be tuned reversibly upon exposure to and removal of CO₂ under mild conditions of temperature and pressure. The equilibrium microstructures of these domains have been characterized by small-angle neutron scattering and demonstrate that control over emulsion morphology (and therefore physicochemical properties such as viscosity) and the breaking of emulsions can be achieved without the need for irreversible changes in system composition or significant energy input.



■ INTRODUCTION

Microemulsions are commercially important systems because they contain precise and thermodynamically stable isotropic nanodomains.¹ Typically, these structural domains are attained by mixing oil and water in the presence of a surfactant, but more recently microemulsions have been formulated using room temperature ionic liquids (ILs) as either the dispersed or continuous phase.^{2,3} ILs are highly tunable and practically nonvolatile solvents, which have already found application in catalysis,⁴ organic synthesis,⁵ and extraction,⁶ and the formation of microemulsions with structured hydrophilic and hydrophobic nanodomains is important in conferring selectivity to reactions and controlling physicochemical properties such as viscosity. The ability to destabilize the microemulsions completely is also vital for isolating products. Conventionally, control of microemulsion stability is achieved by changing the temperature (requiring significant energy input) or through changes in pH, addition of electrolyte or solvent, or saturation with water (each irreversibly altering the composition of the system). A novel approach to avoid energy intensive and irreversible processes has been to employ photoresponsive surfactants, which trigger destabilization upon exposure to UV light,⁷ and CO₂-responsive surfactants, which can act as switchable demulsifiers.⁸ Magnetic microemulsions have also been formulated with magnetic surfactants,^{9,10} and more recently the use of a magnetic ionic liquid as the dispersed phase was demonstrated,¹¹ but there is, as yet, no evidence that macroscopic observations of a magnetic effect are due to changes in microemulsion droplet structure (Supporting Information).

In this paper we demonstrate that reactive ILs can be used to generate reversibly responsive microemulsions and detail the effects of changing solution conditions on structure using small-angle neutron scattering (SANS). The tunable response of microemulsions to CO₂ has been reported before,¹² but such systems have always relied on modification of solvent effects by simple dissolution of CO₂ under pressure (supercritical) rather than through any genuine responsive components. In contrast, the CO₂-responsive microemulsions investigated in this paper undergo reversible chemisorption of CO₂ at ambient temperature and pressure and allow for a nontoxic, affordable, and tunable method to control microemulsion structure and electrostatics.

■ EXPERIMENTAL SECTION

Materials and Synthesis. 1-Butyl-3-methylimidazolium chloride (bmimCl, ≥99%), 1-decanol (98%), 1-chlorohexadecane (≥97%), 1H-1,2,3-triazole (97%), 1-methylimidazole (99%), and cyclohexane (99.5%) were purchased from Sigma-Aldrich and used as received. 1-Butyl-3-methylimidazolium triazolide ([bmim][tria123]) was synthesized by first stirring bmimCl overnight in a strongly basic anion exchange resin suspension (Dowex Monosphere 550A UPW) in a 50:50 (v/v) methanol/water mixture. After filtration of the ion-exchange resin, 1 equiv of 1H-1,2,3-triazole was added to the solution and stirred for 30 min. The product was then obtained by removing the solvent at reduced pressure and drying in vacuo for 24 h. 1-Hexadecyl-3-methylimidazolium chloride (C₁₆mimCl) was synthesized by stirring equimolar amounts of 1-methylimidazole and 1-chlorohexadecane at 130 °C for 24 h. The resulting ionic liquid

Received: February 24, 2014

Revised: March 31, 2014

Published: April 1, 2014

surfactant was recrystallized using tetrahydrofuran and dried in vacuo for 48 h. The synthesized compounds were characterized by NMR, with shifts consistent with expected values. ^1H NMR [bmim][tria123] (300 MHz, methanol- d_4 23 °C): δ 0.90–1.00 (m, 3H), 1.25–1.38 (m, 2H), 1.73–1.85 (m, 2H), 3.82 (s, 3H), 4.06–4.13 (t, 2H), 7.43–7.55 (m, 5H). ^1H NMR $\text{C}_{16}\text{mimCl}$ (300 MHz, methanol- d_4 23 °C): δ 0.85–0.94 (m, 3H), 1.20–1.44 (m, 26H), 1.82–1.95 (m, 2H), 3.92 (s, 3H), 4.16–4.25 (t, 2H), 7.56–7.59 (t, 1H), 7.63–7.66 (t, 1H), 8.95 (s, 1H).

Chemical Adsorption and Desorption. The adsorption of CO_2 in the pure IL was recorded as a function of time at 25 ± 0.05 , 40 ± 0.05 , and 60 ± 0.05 °C under a CO_2 flow rate of 60 mL min^{-1} in a TGA-Q50 (TA Instruments, New Castle, DE). The desorption of the captured CO_2 was measured at the same temperatures with N_2 used as the flowing gas. A typical sample weight in the aluminum pan of the TGA instrument was around 20 mg. Changes in molecular volume on reaction of the anion with CO_2 were estimated with Spartan'06 (Wave function Inc., Irvine, CA) molecular modeling software calculated by the Hartree–Fock method with a 3-21G basis set.

Pseudophase Diagrams. Phase diagrams were produced at 25 ± 0.5 , 40 ± 0.5 , and 60 ± 0.5 °C by titration of a given amount of a mixture of ionic liquid and surfactant-cosurfactant with cyclohexane. The molar ratio of the $\text{C}_{16}\text{mimCl}$ /decanol was maintained at 1:2 in all cases.

CO_2 Response of the Microemulsion. A typical experiment used 10 mL of microemulsion placed in a test tube (10 mm diameter) with a magnetic stir bar and sealed with a septum. The meniscus was marked. A needle piercing the septum was used for pressure release and bone dry gas (CO_2 or N_2) was bubbled through the solution at a rate of 100 mL min^{-1} for 10 min at 25 ± 0.5 °C. At the end of the experiment the small amount ($\phi < 0.02$) of cyclohexane lost through evaporation was replaced.

Solubility of CO_2 in the oil phase (cyclohexane) was estimated from literature values to be around $x_{\text{CO}_2} = 7.5 \times 10^{-4}$ at room temperature and pressure (cf. Supporting Information).

Small-Angle Neutron Scattering (SANS). SANS measurements were performed on the NG-3 (30 m) beamline¹³ at the National Institute of Standards and Technology (NIST) in Gaithersburg, MD. Neutrons with a wavelength of 6 Å were selected, and three sample-detector distances were used to probe a range of wave vectors between 0.004 and 0.4 \AA^{-1} . Data normalization using accepted procedures gave the absolute cross section $I(Q)$ (cm^{-1}) as a function of momentum transfer Q (\AA^{-1}).¹⁴

Samples were prepared using deuterated cyclohexane (scattering length density $\rho = 4.45 \times 10^{10} \text{ cm}^{-2}$) to provide the necessary contrast and were placed in Hellma fused silica cuvettes: path length 1 mm. A low level of residual incoherent scattering was accounted for by a small flat background term in the data analysis. Data were analyzed in absolute units ($I(Q)/\text{cm}^{-1}$) with fitted scale factors consistent with expectations based on sample compositions. Data were analyzed by Porod analysis (details in Supporting Information),¹⁵ while microemulsion structural parameters were extracted from the Teubner–Strey¹⁶ or core–shell¹⁷ models.

RESULTS AND DISCUSSION

The reaction of CO_2 with the aprotic heterocyclic triazolide (tria123) anion was recently reported to exhibit fast binding kinetics.¹⁸ Viscosity remained almost constant upon reaction owing to the lack of hydrogen bonding, while an enhanced physisorption was inferred based on the presence of multiple binding sites. The activation energy of [tria123] was computed to be $E_a = -46.3 \text{ kJ mol}^{-1}$. The CO_2 capacity of 1-butyl-3-methylimidazolium triazolide 1,2,3 or [bmim][tria123] (Figure 1, inset) at 25 °C and 1 bar was determined by thermogravimetric analysis (TGA); the observed weight gain of approximately 11% shown in Figure 1 corresponds to a final mole fraction x_{CO_2} of around 0.36. More than 80% of this

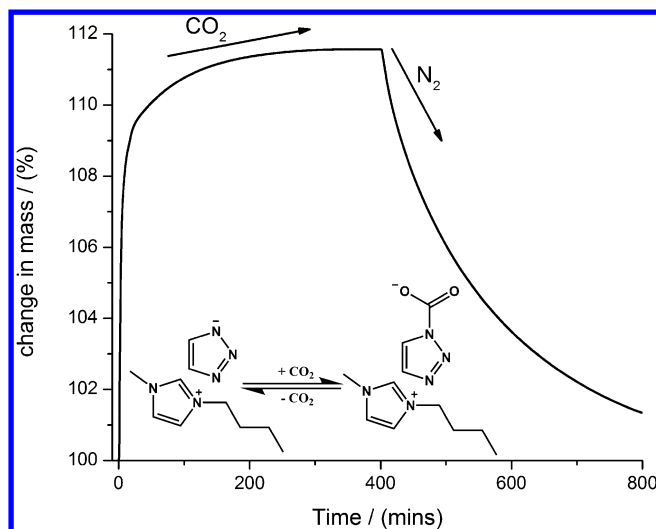


Figure 1. Absorption and desorption of CO_2 in pure IL [bmim]-[tria123] at 25 °C. The specific reaction between the IL and CO_2 is shown.

capacity was attained rapidly and was attributed to chemisorption. On exchange of the flowing gas from CO_2 to N_2 , the CO_2 desorbed completely (Figure 1 and Supporting Information Figure S1). Absorption capacity decreased with increasing temperature (Figure S1), as expected.

The compound [bmim][tria123] was employed as the ionic liquid and cyclohexane as the oil in the formulation of our microemulsion system. The surfactant ionic liquid $\text{C}_{16}\text{mimCl}$, which has been shown to be effective in stabilizing IL-in-oil microemulsions,¹¹ was utilized in this work, with the cosurfactant decanol added to achieve the ultralow surface tensions required for microemulsion formation.

The phase behavior of the pseudoternary system composed of surfactant/cosurfactant at constant molar ratio (1:2), oil, and IL was established at a number of temperatures, as shown in Figure 2 and Figure S2. As in the work of Gradzielski et al.,¹¹ stable microemulsions could only be generated with relatively small amounts of surfactant (mass fraction, $\omega_{\text{surf}} < 0.1$),

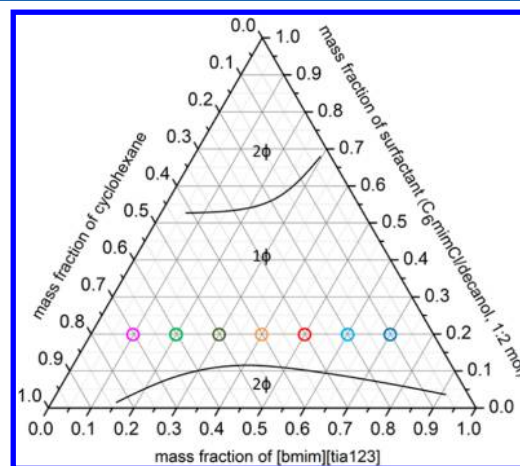


Figure 2. Pseudoternary phase diagram (by mass fraction) for mixtures of [bmim][tria123] and cyclohexane, stabilized by $\text{C}_{16}\text{mimCl}$ and decanol (molar ratio 1:2) as surfactant and cosurfactant, respectively. Colored circles represent composition of samples investigated by SANS (cf. Figure 3).

probably due to the 2-fold presence of the cosurfactant relative to the primary surfactant. The phase diagrams were constructed through visual observation of the large optically clear region characteristic of microemulsion formation. Gels formed when the surfactant concentration was increased to around $\omega_{\text{surf}} = 0.6$ (Figure 2). With increasing temperature, these gel-like systems disappeared almost completely over the composition ranges studied (Figure S2). At low amphiphile concentrations Winsor II systems were evident.

Small-angle neutron scattering (SANS) can give an unambiguous insight into the mesoscopic microemulsion structure. Samples with increasing IL concentration at a constant overall surfactant concentration were selected for study by SANS. The r ratio,¹⁹ where $r = [\text{IL}]/[\text{surfactant}]$, governs the tendency for the IL to disperse within the oil phase due to the influence of the amphiphile and the solvent on interfacial curvature and energy. Figure 3 shows SANS curves

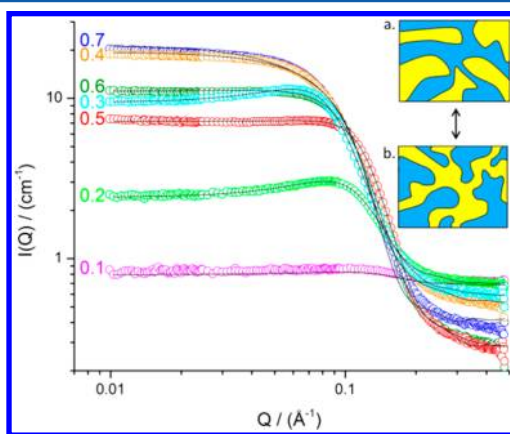


Figure 3. Experimental SANS profiles of bicontinuous samples recorded at 25 °C. Values represent ω_{IL} . Solid lines represent model fits with parameters reported in Table 1. Inset gives a schematic of the bicontinuous microemulsion structure present, which inverts when $\omega_{\text{IL}} = 0.4$ – 0.5 . (a) is rich in oil ($\omega_{\text{IL}} = 0.3$) and r is small; (b) is rich in IL ($\omega_{\text{IL}} = 0.6$) and has larger r values. Curves for $\omega_{\text{IL}} = 0.3, 0.4,$ and 0.5 are fits of the TS model to the data; all others are based on a core–shell model. Error bars not shown for readability but are commensurate with indicated scatter.

for the [bmim][tria123]-in-*d*-cyclohexane microemulsions. It is clear from the scattering profiles in bulk contrast that an increasing ω_{IL} ratio (which corresponds to increasing r) leads to an increase in scattering intensity with the broad structure factor shifting to lower Q and finally, at around $\omega_{\text{IL}} = 0.4$, disappearing. Such patterns have been observed for both conventional and ionic liquid microemulsions and indicate the formation of relatively large domains and bicontinuous structures.²⁰

The Teubner–Strey (TS) phenomenological model¹⁶ accounting for scattering from bicontinuous microemulsions (and other disordered structures) was applied to elucidate quantitative structural information on the microemulsions. The broad peak observed in the scattering intensity distribution, $I(Q)$, may be described by expanding the order parameter of the Landau free energy to give

$$I(Q) = \frac{8\pi c_2 \langle \eta^2 \rangle / \xi_{\text{TS}}}{a_2 - c_1 Q^2 + c_2 Q^4}$$

Here, $\langle \eta^2 \rangle = \varphi_{\text{IL}} \varphi_{\text{o}} \Delta \rho^2$, where φ represents the volume fractions of the domains (ionic liquid and oil) of the bicontinuous structure, and $\Delta \rho$ is the difference in scattering length density between the components, i.e., the contrast between the two phases. The coefficients a_2 , c_1 and c_2 are described in the Supporting Information (Table S1). When $c_1^2 / (4a_2 c_2) < 1$, the inverse Fourier transform of $I(Q)$ leads to the following Debye correlation function

$$g(r) = \frac{d_{\text{TS}}}{2\pi r} e^{-r/\xi_{\text{TS}}} \sin\left(\frac{2\pi r}{d_{\text{TS}}}\right)$$

where d_{TS} represents a quasiperiodic repeat distance or mean domain size and may be determined from

$$d_{\text{TS}} = 2\pi \left[\frac{1}{2} \left(\frac{a_2}{c_1} \right)^{1/2} - \frac{c_1}{4c_2} \right]^{-1/2}$$

The quantity ξ_{TS} is a correlation length, which describes the length scale of the intermediate range fluctuations, and may be calculated from

$$\xi_{\text{TS}} = 2\pi \left[\frac{1}{2} \left(\frac{a_2}{c_2} \right)^{1/2} + \frac{c_1}{4c_2} \right]^{-1/2}$$

The functional form of $g(r)$ illuminates two properties of the bicontinuous microemulsion: the sinusoidal term accounts for the alternating component-rich domains of average size $d/2$, and the exponential term indicates the short-range order among the domains over a distance of about ξ_{TS} .

The aforementioned coefficients are also useful in formulating an amphiphilicity factor $f_a = c_1 / (4a_2 c_2)^{1/2}$. When $f_a \leftarrow 1$, strong amphiphilicity dictates that the microemulsion phase is unstable with respect to the lamellar phase. With lower amphiphilicity, $-1 < f_a < 0$, good microemulsion structures are observed. The spontaneous creation of an interface requires a negative coefficient in the gradient squared term (c_1) and thus a negative f_a , while stability requires a positive higher order term (c_2). These criteria are consistent with strong interfacial correlations, which dominate scattering and produce a peak in the scattering profiles at $Q_{\text{max}} = c_1^{1/2}$.

A second model, that of hard core–shell spherical droplets,¹⁷ was also employed to analyze the data. In this model, the overall scattering intensity is expressed as the product of the form factor $P(Q)$ and a structure factor $S(Q)$

$$I(Q) = NP(Q, R_c, t)S(Q, R_{\text{SH}}, \phi_p)$$

where

$$P(Q) = \frac{\text{scale}}{V_s} \left[3V_c (\rho_c - \rho_s) \frac{[\sin(QR_c) - QR_c \cos(QR_c)]}{(QR_c)^3} + 3V_s (\rho_c - \rho_{\text{solv}}) \frac{[\sin Q(R_c + t) - QR_c \cos Q(R_c + t)]}{(Q(R_c + t))^3} \right]^2 + \text{bkg}$$

Here, scale is a scale factor, V_s is the volume of the outer shell, V_c is the volume of the core, R_c is the radius of the core, ρ_c is the scattering length density (SLD) of the core, ρ_s is the SLD of the shell, ρ_{solv} is the SLD of the solvent, bkg is the background level, t represents shell thickness, and ϕ_p represents the volume fraction of the spheres. The calculated SLDs assumed solid boundaries with no mixing of surfactant with oil or ionic liquid.

$S(Q)$ is given by the structure factor for a hard sphere²¹

Table 1. Fitted Parameters to Microemulsion Structures from SANS^a

ω_{IL}	r ratio	TS model				$\kappa/(k_{\text{B}}T)$	Porod		core-shell model	
		ξ_{TS} (Å)	d_{TS} (Å)	f_a	R_{g} (Å)		R_{c} (Å)	t (Å)	R_{HS} (Å)	
0.1	2.48	13	50	-0.48	0.09		9	10	19	
0.2	4.96	19	65	-0.55	0.09	20	11	13	24	
0.3	7.44	24	87	-0.50	0.12	24	15	18	33	
0.4	9.93	20	104	-0.18	0.11	24	24	12	36	
0.5	12.41	18	72	-0.42	0.13	22	12	11	23	
0.6	14.89	19	82	-0.37	0.14	23	16	11		
0.7	17.37	20	107	-0.15	0.13	25	14	10		

^aTotal radius may be described by adding the core radius with the shell thickness, $R_{\text{HS}} = R_{\text{c}} + t$ when $P(Q)S(Q) = I(Q)$. For the samples containing $\omega_{\text{IL}} = 0.6$ and $\omega_{\text{IL}} = 0.7$ no structure factor ($S(Q)$) was observed, and so this relation does not hold true.

$$S_{\text{HS}}(Q) = \frac{1}{(1 - n_{\text{p}})f(R_{\text{HS}}\phi_{\text{p}})}$$

where the hard-sphere radius R_{HS} is given by $R_{\text{c}} + t$ and n_{p} represents the number density. The hard-sphere potential is a reasonable first approximation for spherical droplets with low attractive interactions.

As with previous studies on ionic liquid-based microemulsions, the quality of the model fit, though always reasonable, depended on the position of the sample within the phase diagram.

For microemulsions with very high ($\omega_{\text{IL}} = 0.5-0.7$) or fairly low IL concentrations ($\omega_{\text{IL}} = 0.1-0.2$) the core-shell model performed better than did the TS model as it assumes a sharp interface between monodisperse compact droplets and the continuous phase. The results compared favorably with those based on the Porod law¹⁵ at large Q with $I(Q) \propto Q^{-4}$ (Table 1). However, for the $\omega_{\text{IL}} = 0.1$ sample the length scale of the system approached that of the local interface and the Porod limit was reached. Generally in the high and low regimes of spherical droplets, core size increased with increasing r and shell thickness remained relatively small as the surfactant headgroup partitioned into the dispersed phase and altered the scattering length density of the system accordingly. It is important to note that scattering profiles for samples $r = 14.89$ and $r = 17.37$ could not be fitted with a hard sphere model as no structure factor could be discerned under these conditions.

For compositions with $\omega_{\text{IL}} = 0.3$ and 0.4 , the TS model proved to be superior to the core-shell description. In this regime, an increasing IL content increased the quasiperiodic distance while ξ_{TS} decreased slightly (Table 1). For all samples it is worth noting that the amphiphilicity factor f_a lay between -1 and 0 , indicating that all microemulsions studied may be considered "good". Importantly, the lower amphiphilicity values at higher r values indicate more structural ordering of the microemulsion droplets.

To corroborate these values, the bending rigidity κ was calculated. The bending rigidity is an elastic modulus of the surface membrane and may be estimated from

$$\frac{\kappa}{k_{\text{B}}T} = \frac{10\xi_{\text{TS}}\sqrt{3\pi}}{64d_{\text{TS}}}$$

The values of κ (Table 1) are quite low, indicating a very soft surfactant interface for bicontinuous phases and microemulsion droplets with extremely low Laplace pressures. For this reason these systems are sensitive to the effects of CO_2 in the IL phase.

After CO_2 was bubbled through the microemulsions for 5 min at room temperature a different picture emerged. The

microemulsions became turbid to the eye, a result of larger droplet formation due to breaking of the microemulsions and a loss of thermodynamic stability (Figure 4, inset). This was

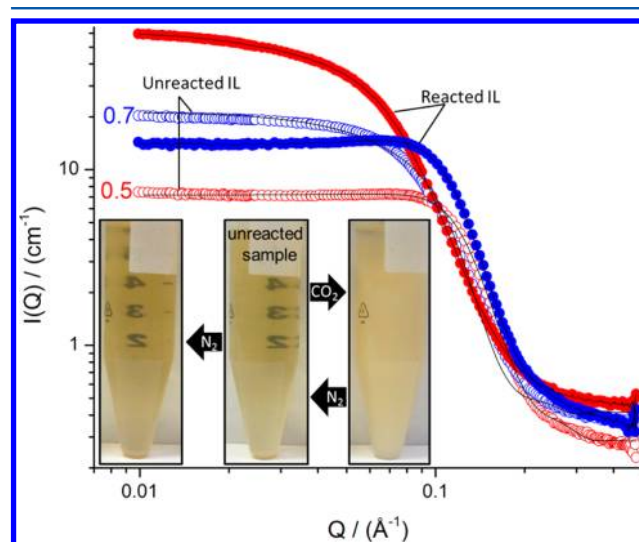


Figure 4. SANS profiles of bicontinuous samples $\omega_{\text{IL}} = 0.5$ (red circles) and $\omega_{\text{IL}} = 0.7$ (blue circles). Open symbols represent unreacted IL, and closed symbols represent samples after bubbling with CO_2 for 5 min at 25°C . Baseline has been corrected. Fitted parameters reported in Table 2. Inset shows change in turbidity corresponding to the breaking of microemulsion structure after bubbling with CO_2 and re-formation of structure on bubbling with N_2 . The bubbling of N_2 through an unadulterated microemulsion sample had no noticeable effect. Error bars not shown for readability but are commensurate with indicated scatter.

partly a result of a slight change in electrostatic interactions and therefore a change in surfactant rigidity, but mainly the result of an increase in the anion volume by almost 50% from around 64 to 94 \AA^3 (from Hartree-Fock calculations). The effect of the change in the anion-cation pair on the Connolly solvent interaction²⁰ should also be considered, but this change is difficult to ascertain through *ab initio* calculations. Importantly the reacted microemulsion could be returned to its clear transparent state on bubbling with N_2 for a significant period of time (>1 h) or on gentle heating. It should be noted that CO_2 absorption in the oil phase was extremely low (Supporting Information).

SANS provided a snapshot of the changing structure of the microemulsion phase on bubbling with CO_2 for a short period of time before phase separation occurred (Table 2, Figure 4, and Figures S4 and S5). The microemulsion at $\omega_{\text{IL}} = 0.1$, which

Table 2. SANS Parameters after Reaction with CO₂ for 5 min at Room Temperature^a

ω_{IL}	r ratio	TS model				$\kappa/(k_{\text{B}}T)$	Porod		core-shell model		
		ξ_{TS} (Å)	d_{TS} (Å)	f_a	R_g (Å)		R_c (Å)	t (Å)	L (Å)	R_{HS} (Å)	
0.1	2.48	11	52	-0.30	0.10		25	0			
0.2	4.96	18	90	-0.25	0.10	24	14	18		32	
0.3	7.44	23	94	-0.41	0.12	23	15	19		34	
0.4	9.93	23	113	-0.23	0.10	27	14	18		32	
0.5	12.41	24	153	-0.02	0.07	29	14	19		32	
0.6	14.89	22	102	-0.31	0.10	27			36		
0.7	17.37	21	80	-0.47	0.13	23	12			27	

^a $\omega_{\text{IL}} = 0.5$ sample fitted as core-shell (cylinder) model.

was initially modeled well as a dispersion of spherical droplets in a continuous phase, could no longer be described by the core-shell structure model, which observation was consistent with a loss of sphericity and the formation of loosely bound aggregates with no defined core. This change in structure may have been due to a lowered amphiphilicity (f_a) of the surfactants. For $\omega_{\text{IL}} = 0.2$ the droplets increased significantly in size and interfacial thickness on exposure to CO₂, which resulted in a decrease in f_a . The TS model applied to the emulsions with $\omega_{\text{IL}} = 0.3$ – 0.4 showed that the quasiperiodic distances increased, which was attributed to an increase in IL volume. For the $\omega_{\text{IL}} = 0.5$ sample, a positive c_1 value was obtained, consistent with a positive f_a and the onset of structural deformation of the microemulsion due to loss of thermal stability. The increase of d_{TS} by around 112% was probably due to the increased molecular volume of the CO₂-IL conjugate. The change at $\omega_{\text{IL}} = 0.6$ was also significant (~24%), but the $\omega_{\text{IL}} = 0.7$ sample was fitted well using a core-shell model with appropriate structure factor, $S(Q)$.

Viscosity also increased on bubbling with CO₂ until a gel-like structure was obtained. Crossing points in the high Q region of the SANS profiles provided evidence of the increasing size of the aggregates, while loss of the structure factor alluded to a transition from core-shell spherical droplets to a true bicontinuous phase, due to a change in molecular binding and in the solvent properties of the ionic liquid, as well as a change in electrostatics that influenced f_a .

CONCLUSIONS

We have introduced a new method for generating stimuli-responsive microemulsions and emulsions simply and inexpensively by using CO₂ and a responsive ionic liquid. Most industrial formulations such as cosmetics, cleaning agents, and pharmaceuticals are already optimized with conventional surfactants, and their replacement with switchable surfactants is often undesirable.²² On the other hand, a shift toward IL formulations is already being considered because of their unique solvent properties and ease with which they may be extracted after use.^{4–6} And in this case, the exploitation of switchable ILs does not limit possibilities due to the immense number of potential IL structures.²³ Moreover, all CO₂ responsive surfactants to date exist in a binary state of being switched “on” or “off”, whereas a significant advantage of the IL system is that CO₂ absorption does not necessarily lead to complete destabilization but may allow for tunable colloidal architectures and give rise to multiple responsive mechanisms. In addition, extra effects may be observable with those ILs that increase dramatically in viscosity upon absorbing CO₂.

Such emulsion systems may be applied to processes such as removal of syngas where the increased interfacial area provided

by microemulsion formation is advantageous. In this respect it is also worth noting that these ILs have much higher absorption capacities toward SO₂ than CO₂.¹⁸

Finally, it may also be propitious to combine the concepts introduced here with the work of Zhang et al. to use supercritical CO₂ as both the continuous phase and a reactant.²⁴

ASSOCIATED CONTENT

Supporting Information

Figures S1–S8 and Table S1. This material is available free of charge via the Internet at <http://pubs.acs.org>.

AUTHOR INFORMATION

Corresponding Author

*E-mail: tahatton@mit.edu (T.A.H.).

Notes

The authors declare no competing financial interest.

ACKNOWLEDGMENTS

We thank Saudi Aramco for funding and the NIST Centre for Neutron Research for beam time and a financial travel grant. This work utilized facilities supported in part by the National Science Foundation under Agreement No. DMR-0944772. The statements, findings, conclusions, and recommendations are those of the authors and do not necessarily reflect the view of NIST

REFERENCES

- (1) Klier, J.; Tucker, C. J.; Kalantar, T. H.; Green, D. P. Properties and applications of microemulsions. *Adv. Mater.* **2000**, *12*, 1751–1757.
- (2) Eastoe, J.; Gold, S.; Rogers, S. E.; Paul, A.; Welton, T.; Heenan, R. K.; Grillo, I. Ionic liquid-in-oil microemulsions. *J. Am. Chem. Soc.* **2005**, *127*, 7302–7303.
- (3) Seth, D.; Chakraborty, A.; Setua, P.; Sarkar, N. Interaction of ionic liquid with water in ternary microemulsions (triton X-100/water/1-butyl-3-methylimidazolium hexafluorophosphate) probed by solvent and rotational relaxation of Coumarin 153 and Coumarin 151. *Langmuir* **2006**, *22*, 7768–7775.
- (4) Moniruzzaman, M.; Kamiya, N.; Nakashima, K.; Goto, M. Water in ionic liquid microemulsions as a new medium for enzymatic reactions. *Green Chem.* **2008**, *10*, 497–500.
- (5) Rao, G. V.; Banerjee, C.; Ghosh, S.; Mandal, S.; Kuchlyan, J.; Sarkar, N. A step toward the development of high-temperature stable ionic liquid-in-oil microemulsions containing double-chain anionic surface active ionic liquid. *J. Phys. Chem. B* **2013**, *117*, 7472–7480.
- (6) Chen, J.; Cao, J.; Gao, W.; Qi, L. W.; Li, P. Environmentally friendly ionic liquid-in-water microemulsions for extraction of hydrophilic and lipophilic components from *Flos Chrysanthemi*. *Analyst* **2013**, *138*, 5933–5941.

- (7) Eastoe, J.; Sanchez-Dominguez, M.; Cumber, H.; Burnett, G.; Wyatt, P. Photoresponsive microemulsions. *Langmuir* **2003**, *19*, 6579–6581.
- (8) Liu, Y.; Jessop, P. G.; Cunningham, M.; Eckert, C. A.; Liotta, C. L. Switchable surfactants. *Science* **2006**, *313*, 958–960.
- (9) Brown, P.; Bushmelev, A.; Butts, C. P.; Cheng, J.; Eastoe, J.; Grillo, I.; Heenan, R. K.; Schmidt, A. M. Magnetic control over liquid surface properties with responsive surfactants. *Angew. Chem., Int. Ed.* **2012**, *51*, 2414–2416.
- (10) Brown, P.; Butts, C. P.; Eastoe, J.; Glatzel, S.; Grillo, I.; Hall, S. H.; Rogers, S.; Trickett, K. Microemulsions as tunable nanomagnets. *Soft Matter* **2012**, *8*, 11609–11612.
- (11) Klee, A.; Prevost, S.; Kunz, W.; Schweins, R.; Kiefer, K.; Gradzielski, M. Magnetic microemulsions based on magnetic ionic liquids. *Phys. Chem. Chem. Phys.* **2012**, *14*, 15355–15360.
- (12) Zhang, J.; Han, B. Supercritical or compressed CO₂ as a stimulus for tuning surfactant aggregations. *Acc. Chem. Res.* **2013**, *46*, 425–433.
- (13) Glinka, C. J.; Barker, J. G.; Hammouda, B.; Krueger, B.; Moyer, J. J.; Orts, W. J. The 30-meter small angle neutron scattering instruments at the National Institute of Standards and Technology. *J. Appl. Crystallogr.* **1998**, *31*, 430–445.
- (14) Kline, S. R. Reduction and analysis of SANS and USANS data using IGOR Pro. *J. Appl. Crystallogr.* **2006**, *39*, 895–900.
- (15) Porod, G.; Koll, Z. *Röntgenkleinwinkelstreuung von dichtgepackten kolloiden Systemen* **1951**, *124*, 83–114.
- (16) Teubner, M.; Strey, R. Origin of the scattering peak in microemulsions. *J. Chem. Phys.* **1987**, *87*, 3195–3200.
- (17) Guinier, A.; Fournet, G. *Small-Angle Scattering of X-Rays*; John Wiley and Sons: New York, 1955.
- (18) Tang, H.; Wu, C. Reactivity of azole anions with CO₂ from the DFT perspective. *ChemSusChem* **2013**, *6*, 1050–1056.
- (19) Winsor, P. A. Hydrotrophy, solubilisation and related emulsification processes. *Trans. Faraday Soc.* **1948**, *44*, 376–398.
- (20) Wellert, S.; Karg, M.; Holderer, O.; Richardt, A.; Hellweg, T. Temperature dependence of the surfactant film bending elasticity in a bicontinuous sugar surfactant based microemulsion: a quasielastic scattering study. *Phys. Chem. Chem. Phys.* **2011**, *13*, 3092–3099.
- (21) Ashcroft, N. W.; Lekner, J. Structure and resistivity of liquid metals. *Phys. Rev.* **1966**, *145*, 83–90.
- (22) Su, X.; Robert, T.; Mercer, S. M.; Humphries, C.; Cunningham, M. F.; Jessop, P. G. A conventional surfactant becomes CO₂-responsive in the presence of switchable water additives. *Chem.—Eur. J.* **2013**, *19*, 5595–601.
- (23) Earle, M. J.; Seddon, K. R. Ionic liquids. Green solvents for the future. *Pure Appl. Chem.* **2000**, *72*, 1391–1398.
- (24) Zhang, J. L.; Han, B. X.; Li, J. S.; Zhao, Y. J.; Yang, G. Y. Carbon dioxide in ionic liquid microemulsions. *Angew. Chem.* **2011**, *123*, 10085–10089.